JACC VOL. 85, NO. 12, 2025

PUBLISHED BY ELSEVIER

Ensemble Deep Learning Algorithm for Structural Heart Disease Screening Using Electrocardiographic Images

PRESENT SHD

Lovedeep S. Dhingra, MBBS,[a] Arya Aminorroaya, MD, MPH,[a] Veer Sangha, BS,[a,b] Aline F. Pedroso, PhD,[a] Sumukh Vasisht Shankar, MS,[a] Andreas Coppi, PhD,[c] Murilo Foppa, MD, PhD,[d] Luisa C.C. Brant, MD, PhD,[e,f] Sandhi M. Barreto, MD, PhD,[g] Antonio Luiz P. Ribeiro, MD, PhD,[e,f] Harlan M. Krumholz, MD, SM,[a,h,i] Evangelos K. Oikonomou, MD, DPhil,[a] Rohan Khera, MD, MS[a,h,j,k]

ABSTRACT

BACKGROUND Identifying structural heart diseases (SHDs) early can change the course of the disease, but their diagnosis requires cardiac imaging, which is limited in accessibility.

OBJECTIVES The purpose of this study was to leverage images of 12-lead electrocardiograms (ECGs) for automated detection and prediction of multiple SHDs using an ensemble deep learning approach.

METHODS We developed a series of convolutional neural network models for detecting a range of individual SHDs from images of ECGs with SHDs defined by transthoracic echocardiograms performed within 30 days of the ECG at the Yale New Haven Hospital (YNHH). SHDs were defined as left ventricular ejection fraction <40%, moderate-to-severe left-sided valvular disease (aortic/mitral stenosis or regurgitation), or severe left ventricular hypertrophy (interventricular septal diameter at end-diastole >1.5 cm and diastolic dysfunction). We developed an ensemble XGBoost model, PRESENT-SHD (Practical scREening using ENsemble machine learning sTrategy for SHD detection), as a composite screen across all SHDs. We validated PRESENT-SHD at 4 U.S. hospitals and the prospective, population-based ELSA-Brasil (Brazilian Longitudinal Study of Adult Health) cohort, with concurrent protocolized ECGs and transthoracic echocardiograms. We also used PRESENT-SHD for risk stratification of new-onset SHD or heart failure (HF) in clinical cohorts and the population-based UK Biobank.

RESULTS The models were developed using 261,228 ECGs from 93,693 YNHH patients and evaluated on a single ECG from 11,023 individuals at YNHH (19% with SHD), 44,591 across external hospitals (20%-27% with SHD), and 3,014 in the ELSA-Brasil (3% with SHD). In the held-out test set, PRESENT-SHD demonstrated an area under the receiver-operating characteristic curve (AUROC) of 0.886 (95% CI: 0.877-894), 90% sensitivity, and 66% specificity. At hospital-based sites, PRESENT-SHD had AUROCs ranging from 0.854 to 0.900, with sensitivities and specificities of 93% to 96% and 51% to 56%, respectively. The model generalized well to ELSA-Brasil (AUROC 0.853 [95% CI: 0.811-0.897], 88% sensitivity, 62% specificity). PRESENT-SHD demonstrated consistent performance across demographic subgroups, novel ECG formats, and smartphone photographs of ECGs from monitors and printouts. A positive PRESENT-SHD screen portended a 2- to 4-fold higher risk of new-onset SHD/heart failure, independent of demographics, comorbidities, and the competing risk of death across clinical sites and UK Biobank, with high predictive discrimination.

CONCLUSIONS We developed and validated PRESENT-SHD, an AI-ECG tool identifying a range of SHD using images of 12-lead ECGs, representing a robust, scalable, and accessible modality for automated SHD screening and risk stratification. (JACC. 2025;85:1302-1313) © 2025 by the American College of Cardiology Foundation.

Listen to this manuscript's audio summary by Editor Emeritus Dr Valentin Fuster on www.jacc.org/journal/jacc.

From the [a]Section of Cardiovascular Medicine, Department of Internal Medicine, Yale School of Medicine, New Haven, Connecticut, USA; [b]Department of Engineering Science, University of Oxford, Oxford, United Kingdom; [c]Center for Outcomes Research and Evaluation, Yale-New Haven Hospital, New Haven, Connecticut, USA; [d]Hospital de Clinicas de Porto Alegre and Post-graduate Program in Cardiology, Universidade Federal do Rio Grande do Sul, Porto Alegre, Brazil; [e]Department of Internal Medicine, Faculdade de Medicina, Universidade Federal de Minas Gerais, Belo Horizonte, Brazil; [f]Telehealth Center and Cardiology Service, Hospital das Clínicas, Universidade Federal de Minas Gerais, Belo Horizonte, Brazil; [g]Department of Preventive Medicine, School of Medicine, Faculdade de Medicina, Universidade Federal de Minas Gerais, Belo Horizonte, Brazil; [h]Center for

ISSN 0735-1097/$36.00 https://doi.org/10.1016/j.jacc.2025.01.030

Structural heart diseases (SHDs) represent a spectrum of prevalent cardiac disorders with a long presymptomatic course and with substantially elevated risk of heart failure (HF) and premature death.[1] The detection of these disorders has traditionally required advanced cardiac imaging, including echocardiography and cardiac magnetic resonance imaging, which are resource-intensive and, therefore, not suitable for large-scale disease screening.[2,3] Consequently, these conditions are often diagnosed after the development of clinical symptoms, leading to poor health outcomes.[4-6] Moreover, there are no strategies to identify individuals at risk of developing SHDs, despite the presence of evidence-based interventions that can alter the course of patients.[6-8] Thus, there is an urgent need for the development of an automated, accessible, and scalable strategy for the screening and risk stratification of SHDs.[1,9]

SEE PAGE 1314

Previously, applications of artificial intelligence for electrocardiograms (AI-ECG) have shown potential to detect signatures of SHDs.[10-18] A key challenge of AI-ECG models in detecting specific cardiac disorders using ECGs is the low precision driven by the low prevalence of individual disorders.[10-12] To overcome this limitation, ensemble models for detecting a composite of multiple SHDs have been proposed.[19] Nonetheless, these models use raw ECG voltage data as inputs, which are inaccessible to clinicians at the point of care and often require modifications to the technical infrastructure to account for vendor-specific data formats.[19] This precludes the widespread use of AI-ECG approaches for broad cardiovascular screening, because these data integrations are not commonly available. Further, most AI-ECG approaches focus on cross-sectional detection and do not quantify the risk of new-onset disease in those without SHD, which would identify a group for continued monitoring. Thus, there is a critical unmet need for an AI-ECG-based strategy to enable cross-sectional detection and longitudinal prediction of multiple SHDs simultaneously using ubiquitous, interoperable, and accessible data input in the form of ECG images.

In this study, we report the development and multinational validation of an ensemble deep learning approach that uses an image of a 12-lead ECG, independent of the format, for the accurate detection and prediction of multiple SHDs.

METHODS

The Yale Institutional Review Board approved the study protocol and waived the need for informed consent because the study involves secondary analysis of preexisting data. An online version of the model is publicly available for research use.[20]

DATA SOURCES. For model development, we included data from the Yale New Haven Hospital (YNHH) during 2015 to 2023. YNHH is a large 1,500-bed tertiary medical center that provides care to a diverse patient population across Connecticut. For external validation of our approach to detect SHDs, we included multiple clinically and geographically diverse cohorts: 1) 4 distinct community hospitals in the Yale-New Haven Health System: the Bridgeport Hospital, Greenwich Hospital, Lawrence + Memorial Hospital, and Westerly Hospital; and 2) a community-based cohort of individuals in Brazil with protocolized concurrent ECG and transthoracic echocardiogram (TTE) assessments: the ELSA-Brasil study.

To evaluate the longitudinal prediction of SHD in people without baseline disease, in addition to serial monitoring data from hospitals in the Yale-New Haven Health System, we included data from the UK Biobank (UKB). UKB is the largest population-based cohort with protocolized ECG assessments and clinical encounters derived from the integrated EHR of the National Health Service in the United Kingdom.

ABBREVIATIONS AND ACRONYMS

AR = aortic regurgitation

AS = aortic stenosis

AUPRC = area under the precision-recall curve

AUROC = area under the receiver-operating characteristic curve

CNN = convolutional neural network

ECG = electrocardiogram

HF = heart failure

LVEF = left ventricular ejection fraction

LVSD = left ventricular systolic dysfunction

MR = mitral regurgitation

NPV = negative predictive value

PPV = positive predictive value

SHD = structural heart disease

sLVH = severe left ventricular hypertrophy

TTE = transthoracic echocardiogram

XGBoost = extreme gradient boosting

YNHH = Yale New Haven Hospital

Outcomes Research and Evaluation (CORE), Yale New Haven Hospital, New Haven, Connecticut, USA; [i]Department of Health Policy and Management, Yale School of Public Health, New Haven, Connecticut, USA; [j]Section of Biomedical Informatics and Data Science, Yale School of Medicine, New Haven, Connecticut, USA; and the [k]Section of Health Informatics, Department of Biostatistics, Yale School of Public Health, New Haven, Connecticut, USA.

The authors attest they are in compliance with human studies committees and animal welfare regulations of the authors' institutions and Food and Drug Administration guidelines, including patient consent where appropriate. For more information, visit the Author Center.

Manuscript received October 7, 2024; revised manuscript received January 3, 2025, accepted January 22, 2025.

CENTRAL ILLUSTRATION **PRESENT-SHD Study Design and Key Findings**

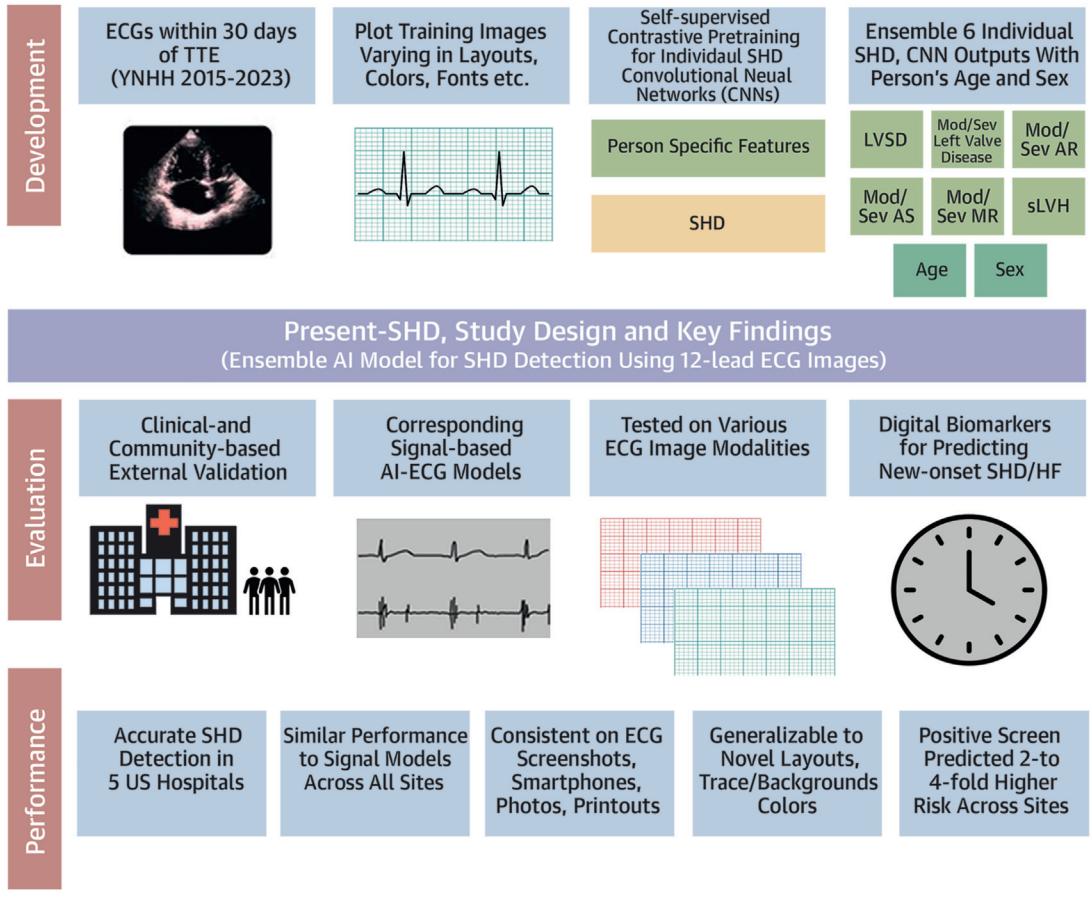

Dhingra LS, et al. JACC. 2025;85(12):1302–1313.

AR = aortic regurgitation; AS = aortic stenosis; CNN = convolutional neural network; ECG = electrocardiogram; HF = heart failure; LVSD = left ventricular systolic dysfunction; SHD = structural heart diseases; sLVH = severe left ventricular hypertrophy; TTE = transthoracic echocardiogram; XGBoost = extreme gradient boosting; YNHH = Yale New Haven Hospital.

An overview of all data sources is included in the Supplemental Methods.

STUDY POPULATION FOR SHD DETECTION. At YNHH, we identified all adults (age ≥18 years) who underwent a 12-lead ECG within 30 days before or after a TTE, excluding those with prior cardiac surgery to replicate the intended use of these models in a screening setting (**Central Illustration**, Supplemental Figure 1). In the internal validation and internal hold-out test sets, and all external validation sites, one ECG was randomly selected from one or more ECGs performed within 30 days of a TTE for each individual. In ELSA-Brasil, all participants who underwent both ECG and TTE at their baseline study visit were included.

SHD OUTCOME. The study outcome of SHD was defined as any left ventricular systolic dysfunction (LVSD), moderate-or-severe left-sided valve disease, or severe left ventricular hypertrophy (sLVH). All conditions were ascertained based on the interpretation of TTE by board-certified cardiologists according to the American Society of Echocardiography guidelines.[21] Echocardiography variables were available in tabular format, obviating manual ascertainment. The left ventricular ejection fraction (LVEF) was primarily measured as a continuous variable using the biplane method. When the LVEF measurement using the biplane method was unavailable, measurements using the 3-dimensional or visual estimation methods were used. LVSD was defined as an LVEF <40%. Left-sided valve diseases included aortic stenosis (AS),

aortic regurgitation (AR), mitral regurgitation (MR), or mitral stenosis, graded as mild to moderate, moderate, moderate to severe, or severe, based on established echocardiographic guidelines.[22,23] We defined sLVH by a combination of an interventricular septal diameter at end-diastole of >15 mm, along with moderate to severe (grades II and III) LV diastolic dysfunction.[24]

SIGNAL PROCESSING AND IMAGE GENERATION. We used a strategy for developing models that can detect SHD from images from ECGs regardless of their layout. This was done using a custom waveform plotting strategy where ECG signals are processed and plotted as images in a format randomly chosen from 2,880 formats, encompassing variations in lead layout, trace and background color, lead label font, size and position, and grid and signal line width (Supplemental Figure 2). We also included nonconventional variations in ECG lead placements, with the chest leads on the left and limb leads on the right side of the plotted ECGs. The plotted signals were processed using a standard preprocessing strategy described previously (and included in the Supplemental Methods). For evaluation, ECG images were plotted in standard clinical layout from signal waveform data, with a voltage calibration of 10 mm/mV, with the limbs and precordial leads arranged in 4 columns of 2.5 seconds each, representing leads I, II, and III; aVR, aVL, and aVF; V_1, V_2, and V_3; and V_4, V_5, and V_6 (Supplemental Figure 3). A 10-second recording of the lead I signal was included as a rhythm strip. We further evaluated the model on 4 novel image formats that were not encountered during model training (Supplemental Methods, Supplemental Figure 4). All images were converted to greyscale and down-sampled to 300 × 300 pixels using Python Image Library.[25] Examples of ECG images used for model training and evaluation are presented in Supplemental Appendix 2.

MODEL DEVELOPMENT FOR INDIVIDUAL SHDs. We trained 6 independent convolutional neural network (CNN) models to detect individual components of SHD (**Central Illustration**). We randomly divided individuals at YNHH into training, validation, and test sets (85:5:10) without any patient spanning these sets (Supplemental Figure 1). We retained multiple ECGs per person in the training set to ensure the adequacy of training data. However, in evaluating the model in the internal validation, held-out test, and external validation sets, only 1 ECG was randomly chosen for every individual. Of note, none of the patients in the external validation sets were in the model development population.

We used CNN models built upon the EfficientNet-B3 architecture, which has 384 layers and over 10 million trainable parameters.[11,26] To enable label-efficient model development, we initialized the CNNs with weights from a model pretrained to recognize individual patient-specific patterns in ECGs, independent of their interpretation, using a self-supervised, contrastive learning framework (**Figure 1**).[27] None of the ECGs on the self-supervised pretraining task represented individuals in the SHD model development.

Each ECG in the training set was plotted using one of the randomly assigned plotting formats described in the previous text. We used an Adam optimizer, gradient clipping, and a minibatch size of 128 throughout training, with sequential unfreezing of the final layers (learning rate, 0.001), and all layers (learning rate, 10^{-5}), with training stopped when validation loss did not improve in 5 consecutive epochs. A custom class-balanced loss function (weighted binary cross-entropy) based on the effective number of samples was used, given the case and control imbalance.

The CNNs for the individual components of SHD had the same model backbone but differed in the populations for training. Five of the 6 models, specifically for those detecting LVSD, the presence of any moderate to severe left-sided valvular heart diseases, and those for moderate-to-severe AR, AS, or MR, were trained using all ECGs in the training set, spanning those with and without each disease. However, given the low prevalence of sLVH (<1%), we age- and sex-matched case and control subjects for model development. Each case, representing an ECG corresponding to an individual with sLVH, was matched to 10 control ECGs without sLVH from someone of the same sex and within 5 years of the case. These individual models were combined into an ensemble model to detect the presence of any SHD. As a sensitivity analysis, we used the same training strategy and model architecture to develop a classifier CNN model directly detecting the presence of SHD. For each SHD component, we also trained corresponding signal-based models within the same label and training population (Supplemental Methods).

ENSEMBLE LEARNING STRATEGY. Following CNN development, output probabilities from the 6-component SHD CNN models, along with a person's age and sex, were used as input features for an extreme gradient boosting (XGBoost) model, PRESENT-SHD (Practical scREening using ENsemble machine learning sTrategy for SHD detection)

FIGURE 1 Model Development Strategy

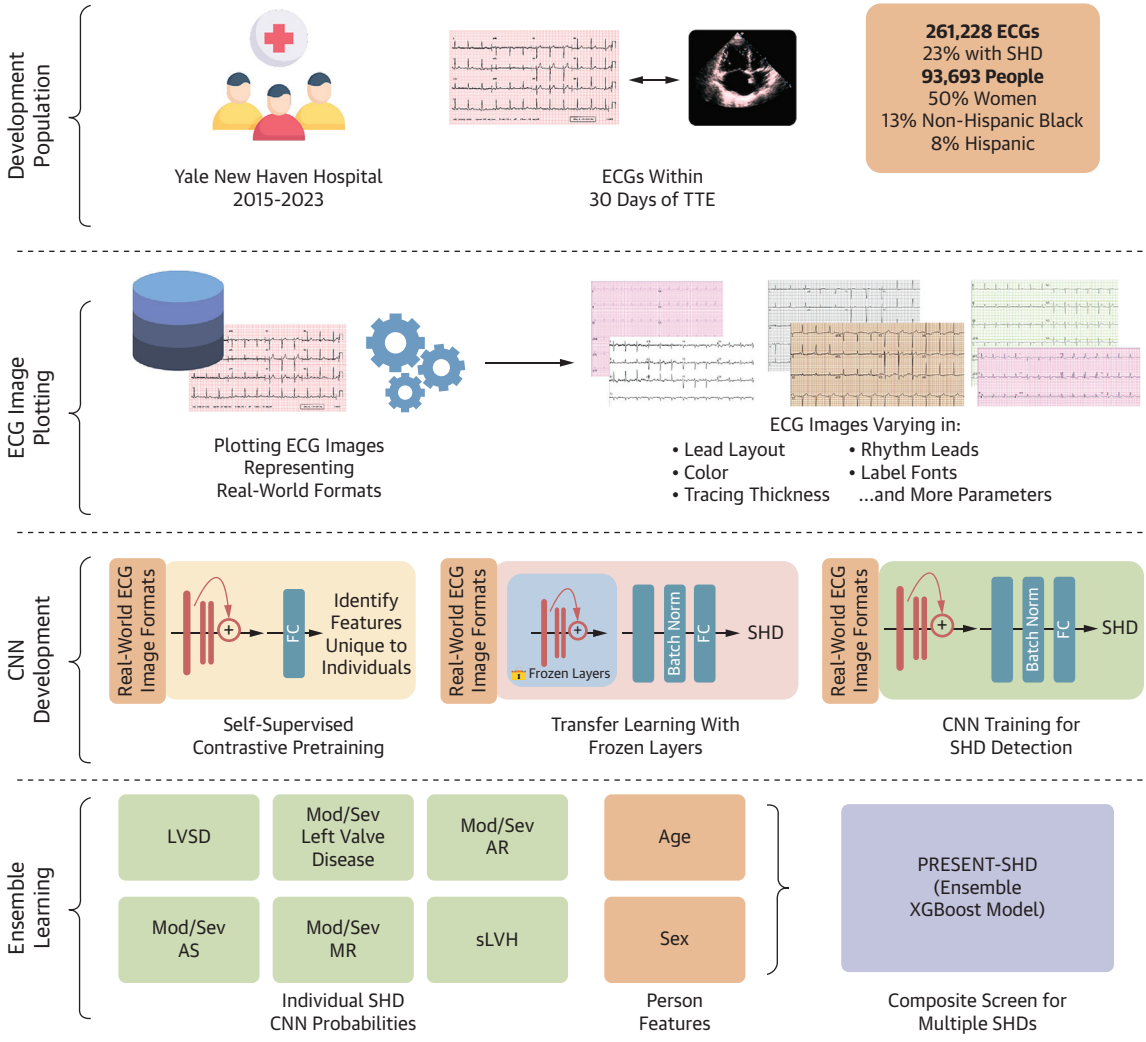

AR = aortic regurgitation; AS = aortic stenosis; CNN = convolutional neural network; ECG = electrocardiogram; FC = fully-connected layers; LVSD = left ventricular systolic dysfunction; MR = mitral regurgitation; SHD = structural heart diseases; sLVH = severe left ventricular hypertrophy; TTE = transthoracic echocardiogram; XGBoost = extreme gradient boosting.

(Figure 1). The XGBoost model was exclusively trained using data from the same training sets as the CNN models. Before being included as features, age and the CNN model output probabilities were standardized to a mean of 0 and a variance of 1 to improve learning stability and ensure consistent feature contribution across different data sets. The standardization algorithm was derived based on the distribution of these variables in the training set and was applied for inference across all other data sets, including internal validation, testing, and external validation sets.

MODEL EVALUATION ON SCREENSHOTS AND SMARTPHONE PHOTOGRAPHS OF ECGs. To evaluate model performance across different strategies for obtaining images in the real world, we selected a random subset of 100 ECGs from the held-out test set. From the EHR, we identified the PDFs for these ECGs and saved screenshots to reflect the exact images used during clinical care. We then photographed the ECGs from a laptop screen displaying them. We also printed them on A4 sheets and photographed them using default camera settings on 3 different smartphones (Supplemental Figure 5, Supplemental Methods).

Finally, we applied the 6 SHD-component CNNs and the PRESENT-SHD model to these screenshots and smartphone photographs (Supplemental Appendix 2), compared the predictions with the images of the same ECGs plotted in the standard format, and evaluated performance for SHD detection.

PREDICTION OF NEW-ONSET SHD. To evaluate the use of the model for stratifying the risk of new-onset disease across data sources, we identified a population without evidence of SHD or HF at baseline. In YNHH, we identified the first recorded encounter for all individuals within the EHR and instituted a 1-year blanking period to define prevalent diseases (Supplemental Figure 6). Among 204,530 patients with ECGs following a 1-year blanking period, we excluded 6,909 individuals with prevalent SHD, 1,197 with a prior valvular repair or replacement procedure, and 13,632 with prevalent HF (Supplemental Table 1). Those included in the model training set (n = 55,245) were also excluded from this analysis. We used a similar strategy across the hospital-based external validation sites to identify patients at risk for new-onset disease—a 1-year blanking period to identify prevalent diseases and exclude those with prevalent SHD/HF or prior valvular procedures. Across sets, new-onset SHD/HF was defined as the first occurrence of any SHD detected on the TTE, any valvular replacement or repair procedure, or hospitalization with HF. Data were censored at death or loss to follow-up.

Further, we identified participants with ECGs in the UKB. We used the national EHR linkage to identify those who had not undergone any hospitalizations with HF and had not undergone valvular procedures before their baseline ECG. We followed these individuals until their first encounter with an SHD or HF diagnosis code, or a left-sided valve replacement or repair procedure (Supplemental Table 1).

STATISTICAL ANALYSIS. We reported continuous variables as median (Q1-Q3) and categorical variables as counts and percentages. Model performance for detecting SHD was reported as area under the receiver-operating characteristic curve (AUROC) and area under the precision-recall curve (AUPRC), with 95% CIs for these computed using bootstrapping with 1,000 iterations. Additional performance measures included sensitivity, specificity, positive predictive value (PPV), negative predictive value (NPV), and F1 score with 95% CIs using the SE formula for proportion. Finally, we calculated the model's PPV in simulated screening scenarios with different prevalences of composite SHD using the model's sensitivity and specificity corresponding to the probability threshold with sensitivity above 90% in the internal validation set.

Among those without SHD at baseline, the predictive role of PRESENT-SHD for new-onset SHD/HF was evaluated in age- and sex-adjusted Cox proportional hazard models. The time-to-first SHD/HF event was the dependent variable and the PRESENT-SHD-based screen status—presumably "false positive" or "true negative" status—was the key independent variable. Further, to account for the competing risk of death while evaluating new-onset SHD, we used age- and sex-adjusted multioutcome Fine-Gray subdistribution hazard models.[28,29] The discrimination of the model for SHD prediction was assessed using Harrell's C-statistic.[30,31] The statistical analyses were 2-sided, and the significance level was set at 0.05. Analyses were executed using Python 3.11.2 and R version 4.2.0. Our study follows the Transparent Reporting of a multivariable prediction model for Individual Prognosis Or Diagnosis + Artificial Intelligence (TRIPOD + AI) checklist from the EQUATOR network (Supplemental Table 2).[32]

RESULTS

STUDY POPULATION. There were 261,228 ECGs from 93,693 unique patients in the training set, and the validation and internal held-out test sets had a single ECG per person from 5,512 and 11,023 patients, respectively (Supplemental Figure 1). The development population (model training and validation sets) had a median age of 67.8 years (Q1-Q3: 56.1-78.3 years), 49,947 (50.3%) were women, 13,383 (13.8%) were non-Hispanic Black, and 7,754 (8.1%) were Hispanic (Supplemental Table 3). In the development population, 60,096 (22.5%) ECGs were paired with TTEs with an SHD, including 25,552 (9.5%) with LVSD, 42,989 (16.1%) with moderate or severe left-sided valvular disease, and 1,004 (0.4%) with sLVH.

At the external hospital sites, 18,222 patients at Bridgeport Hospital, 4,720 patients at Greenwich Hospital, 17,867 patients at Lawrence + Memorial Hospital, and 3,782 patients from Westerly Hospital were included (Supplemental Figure 1), with 44,591 ECGs, randomly 1 chosen per person, across these sites for model evaluation. Across hospital sites, the median age at ECG ranged from 66 to 74 years, with cohorts comprising 48.3% to 50.5% women, 1.5% to 19.4% Black, and 1.4% to 15.9% Hispanic individuals. The distribution of SHDs across these cohorts is described in Supplemental Table 4.

Of the 15,105 participants in ELSA-Brasil, 3,014 who underwent ECG and TTE during their baseline visit were included. The median age of the cohort was

TABLE 1 Performance Metrics for Detecting Structural Heart Disease Across Demographic Subgroups in the Held-Out Test Set

Subgroup	Total Number	Diagnostic OR (95% CI)	AUROC (95% CI)	AUPRC (95% CI)	F1 Score	Prevalence, %	Sensitivity, % (95% CI)	Specificity, % (95% CI)	PPV, % (95% CI)	NPV, % (95% CI)
Overall	6,203	17.2 (14.7-20.1)	0.886 (0.877-0.894)	0.807 (0.791-0.823)	0.700	33.60	89.8 (89.0-90.5)	66.2 (65.0-67.4)	57.4 (56.1-58.6)	92.8 (92.1-93.4)
Age ≥65 y	2,897	8.0 (6.1-10.5)	0.822 (0.807-0.838)	0.839 (0.820-0.857)	0.735	53.20	95.7 (94.9-96.4)	26.6 (25.0-28.2)	59.7 (57.9-61.5)	84.3 (83.0-85.7)
Age <65 y	3,306	16.2 (13.1-20.2)	0.873 (0.856-0.889)	0.679 (0.641-0.716)	0.595	16.50	73.2 (71.7-74.7)	85.6 (84.4-86.8)	50.1 (48.4-51.8)	94.2 (93.4-95.0)
Women	3,150	17.5 (14.1-21.7)	0.884 (0.873-0.896)	0.778 (0.752-0.804)	0.689	30.80	88.5 (87.3-89.6)	69.5 (67.9-71.1)	56.4 (54.7-58.1)	93.1 (92.2-94.0)
Men	3,052	16.7 (13.3-20.9)	0.886 (0.874-0.898)	0.830 (0.810-0.851)	0.710	36.50	90.9 (89.9-92.0)	62.4 (60.7-64.2)	58.2 (56.4-59.9)	92.3 (91.3-93.2)
Non-Hispanic White	3,966	16.7 (13.7-20.5)	0.882 (0.871-0.892)	0.824 (0.805-0.841)	0.711	37.40	91.7 (90.9-92.6)	60.2 (58.7-61.7)	58.0 (56.4-59.5)	92.4 (91.6-93.2)
Non-Hispanic Black	834	17.2 (11.4-25.9)	0.877 (0.852-0.902)	0.774 (0.724-0.823)	0.697	31.50	87.8 (85.6-90.1)	70.4 (67.3-73.5)	57.8 (54.4-61.1)	92.6 (90.9-94.4)
Hispanic	537	15.8 (9.7-25.8)	0.882 (0.846-0.916)	0.786 (0.720-0.844)	0.666	25.50	81.0 (77.7-84.3)	78.8 (75.3-82.2)	56.6 (52.4-60.8)	92.4 (90.1-94.6)
Others	866	18.1 (11.9-27.5)	0.893 (0.868-0.918)	0.740 (0.668-0.803)	0.648	23.10	84.0 (81.6-86.4)	77.5 (74.7-80.3)	52.8 (49.5-56.2)	94.2 (92.6-95.7)

AUPRC = area under the precision-recall curve; AUROC = area under the receiver-operating characteristic curve; NPV = negative predictive value; PPV = positive predictive value.

62.0 years (Q1-Q3: 57.0-67.0 years), 1,596 (53.0%) were women, 1,661 (55.1%) were White, 455 (15.1%) were Black, and 753 (25.0%) were Pardo (or mixed race) individuals. A total of 88 (2.9%) individuals had SHD, with 37 (1.2%) with LVSD, 55 (1.8%) with moderate or severe left-sided valvular disease, and 6 (0.2%) with sLVH (Supplemental Table 4).

DETECTION OF SHD. The ensemble XGBoost model, PRESENT-SHD, demonstrated an AUROC of 0.886 (95% CI: 0.877-0.894) and an AUPRC of 0.807 (95% CI: 0.791-0.823) for the detection of the composite SHD outcome in the held-out test set (**Table 1**). At the probability threshold for sensitivity above 90% in the internal validation set, the model had a sensitivity of 89.8% (95% CI: 89.0%-90.5%), specificity of 66.2% (95% CI: 65.0%-67.4%), PPV of 57.4% (95% CI: 56.1%-58.6%), and NPV of 92.8% (95% CI: 92.1%-93.4%) for detecting SHD in the held-out test set in YNHH (**Table 2**, Supplemental Figure 7). PRESENT-SHD performed consistently across subgroups of age, sex, race, and ethnicity (**Table 1**), and generalized well to novel ECG formats not encountered during training (Supplemental Table 5). Moreover, the model had consistent performance across subsets where TTEs were performed before, on the same day as, or after the ECG (Supplemental Table 6) and had high discrimination for detecting the severe SHD phenotype (LVSD, severe left-sided valve disease, or sLVH) (Supplemental Figure 8). Notably, the performance of PRESENT-SHD was higher than the CNN models trained to directly detect SHD and other XGBoost ensemble strategies (Supplemental Tables 7 and 8).

PRESENT-SHD performance was similar to the corresponding signal-based model for detecting SHD (Supplemental Table 9). Across ECG screenshots and smartphone photographs of monitors and printouts, the model demonstrated high agreement with plotted images (Pearson correlation coefficients, 0.959-0.977) (Supplemental Figure 9) and consistent performance across all image types (AUROCs: plotted images, 0.939 [95% CI: 0.887-0.976]; ECG screenshots, 0.934 [95% CI: 0.885-0.973]; Smartphone photographs of computer monitors, 0.932 [95% CI: 0.878-0.970]; Smartphone photographs of printouts, 0.924 [95% CI: 0.866-0.970]) (Supplemental Table 10).

Further, PRESENT-SHD generalized well to the external validation cohorts at Bridgeport (AUROC: 0.854 [95% CI: 0.847-0.862]), Greenwich (AUROC: 0.900 [95% CI: 0.888-0.913]), Lawrence + Memorial (AUROC: 0.871 [95% CI: 0.864-0.878]), and Westerly (AUROC: 0.887 [95% CI: 0.874-0.902]) Hospitals, with sensitivities and specificities ranging from 88% to 96% and 51% to 66%, respectively. PRESENT-SHD also generalized well to the population-based ELSA-Brasil, with an AUROC of 0.853 (95% CI: 0.811-0.897) and a sensitivity and specificity of 87.5% and 61.9%, respectively (**Table 2**, Supplemental Table 11). Across validation sites, model performance was consistent across demographic subgroups (Supplemental Tables 12 to 16). The F1 scores, PPVs, and NPVs for a range of putative prevalences of SHDs representing different screening scenarios are presented in Supplemental Table 17.

DETECTION OF INDIVIDUAL DISEASES. The models for LVSD, moderate or severe valvular disease, and sLVH had AUROCs of 0.914 (95% CI: 0.904-0.924), 0.805 (95% CI: 0.793-0.817), and 0.903 (95% CI: 0.850-0.946), respectively (**Figure 2**). The performance of

TABLE 2 Model Performance Characteristics for PRESENT-SHD for Detection of Structural Heart Disease Across the Held-Out Test Set and External Validation Cohorts

Cohort Type	Site Name	Total Number	Diagnostic OR (95% CI)	AUROC (95% CI)	AUPRC (95% CI)	F1 Score	Prevalence, %	Sensitivity, % (95% CI)	Specificity, % (95% CI)	PPV, % (95% CI)	NPV, % (95% CI)
Held-out test set	Yale New Haven Hospital	6,203	17.2 (14.7-20.1)	0.886 (0.877-0.894)	0.807 (0.791-0.823)	0.700	33.60	89.8 (89.0-90.5)	66.2 (65.0-67.4)	57.4 (56.1-58.6)	92.8 (92.1-93.4)
External validation											
Hospital sites	Bridgeport Hospital	8,944	14.8 (12.9-16.9)	0.854 (0.847-0.862)	0.834 (0.823-0.845)	0.751	46.60	93.2 (92.6-93.7)	52.0 (51.0-53.1)	62.9 (61.9-63.9)	89.7 (89.1-90.3)
	Greenwich Hospital	2,271	30.6 (22.2-42.1)	0.900 (0.888-0.913)	0.894 (0.878-0.910)	0.798	49.80	96.0 (95.2-96.8)	55.9 (53.9-58.0)	68.3 (66.4-70.2)	93.4 (92.4-94.4)
	Lawrence + Memorial Hospital	11,447	16.0 (14.0-18.2)	0.871 (0.864-0.878)	0.771 (0.757-0.784)	0.643	31.50	92.5 (92.0-93.0)	56.4 (55.5-57.3)	49.3 (48.4-50.3)	94.3 (93.8-94.7)
	Westerly Hospital	1,843	19.9 (14.5-27.3)	0.887 (0.874-0.902)	0.906 (0.890-0.922)	0.810	55.60	95.1 (94.1-96.1)	50.5 (48.3-52.8)	70.6 (68.6-72.7)	89.2 (87.8-90.6)
Population-based cohort	ELSA-Brasil	2,988	11.4 (6.0-21.5)	0.853 (0.811-0.897)	0.354 (0.253-0.460)	0.121	2.90	87.5 (86.3-88.7)	61.9 (60.2-63.6)	6.5 (5.6-7.4)	99.4 (99.1-99.7)

ELSA-Brasil = Brazilian Longitudinal Study of Adult Health; other abbreviations as in Table 1.

CNN models for individual valvular heart diseases varied, with an AUROC of 0.722 (95% CI: 0.784-0.824) for moderate or severe AR, 0.804 (95% CI: 0.784-0.824) for AS, and 0.792 (95% CI: 0.776-0.807) for MR. The CNN model AUPRCs varied with individual disease prevalence (Supplemental Tables 18 to 23). The performance for individual disease CNNs was consistent across external validation cohorts (Supplemental Figure 10, Supplemental Tables 18 to 23) and real-world ECG image modalities (Supplemental Table 24).

PREDICTION OF SHD AND CARDIOVASCULAR RISK. Of the 127,547 individuals at risk in YNHH, 5,346 (4.2%) had new-onset SHD/HF over a median of 4.0 years (Q1-Q3: 1.7-6.4 years) of follow-up. Across the hospital-based external validation sites, there were 63,748 individuals without SHD/HF at baseline and 4,593 (7.2%) developed incident SHD/HF over a median of 3.1 years (Q1-Q3: 1.3-5.0 years) of follow-up (Supplemental Table 25). In UKB, 413 (1.0%) of 41,800 individuals developed SHD/HF over 3.0 years (Q1-Q3: 2.1-4.5 years) of follow-up.

A positive PRESENT-SHD screen portended a 4-fold higher risk of new-onset SHD/HF in YNHH (age- and sex-adjusted HR [aHR]: 4.28 [95% CI: 3.95-4.64], Harrell's C-statistic, 0.823 [95% CI: 0.817-0.828]) and every 10% increment in model probability was progressively associated with a 36% higher hazard for incident SHD/HF (aHR: 1.36 [95% CI: 1.35-1.38]). A similar pattern was observed across all external validation hospital sites (Supplemental Tables 26 and 27). This association remained consistent after adjusting for comorbidities at baseline and the competing risk of death (Supplemental Table 26).

In the UKB, a positive vs negative PRESENT-SHD screen was associated with twice the hazard of developing SHD/HF (aHR: 2.39 [95% CI: 1.87-3.04], Harrell's C-statistic, 0.754 [95% CI: 0.728-0.780]). Across all sites, higher model probabilities were associated with progressively higher risk of new-onset SHD/HF (**Figure 3**, Supplemental Table 28).

DISCUSSION

We developed and validated PRESENT-SHD, an ensemble deep learning model that uses an ECG image as the input to detect a range of SHDs. PRESENT-SHD had excellent performance in detecting SHDs across 5 distinct U.S. hospitals with unique patients and in a population-based cohort study from Brazil. Model performance was consistent across demographic subgroups and similar to the corresponding signal-based models. Additionally, PRESENT-SHD maintained high performance when tested on novel ECG formats, screenshots of ECGs in the EHR, as well as smartphone photographs of ECGs captured from laptop monitors and printouts. Further, in individuals without SHD at baseline, PRESENT-SHD identified those with an up to 4-fold higher risk of developing new-onset SHD/HF, across both health system-centered cohorts in the United States and in a community-based cohort in the United Kingdom. The model was well calibrated to the risk of new-onset disease, such that higher PRESENT-SHD probabilities were associated with progressively higher risk of developing SHD/HF. Thus, an image-based AI-ECG approach is a scalable and accessible strategy for screening for SHDs and identifying those at high risk for developing SHDs.

Prior studies have reported the use of deep learning on 12-lead ECGs to detect individual structural cardiovascular conditions, including LVSD,[10,11,13] hypertrophic cardiomyopathy,[16,33,34] cardiac amyloidosis,[35,36] AS,[12] among others.[15,36-38]

FIGURE 2 Model Discrimination for the Detection of Composite SHD and Individual Components in the Held-Out Test Set

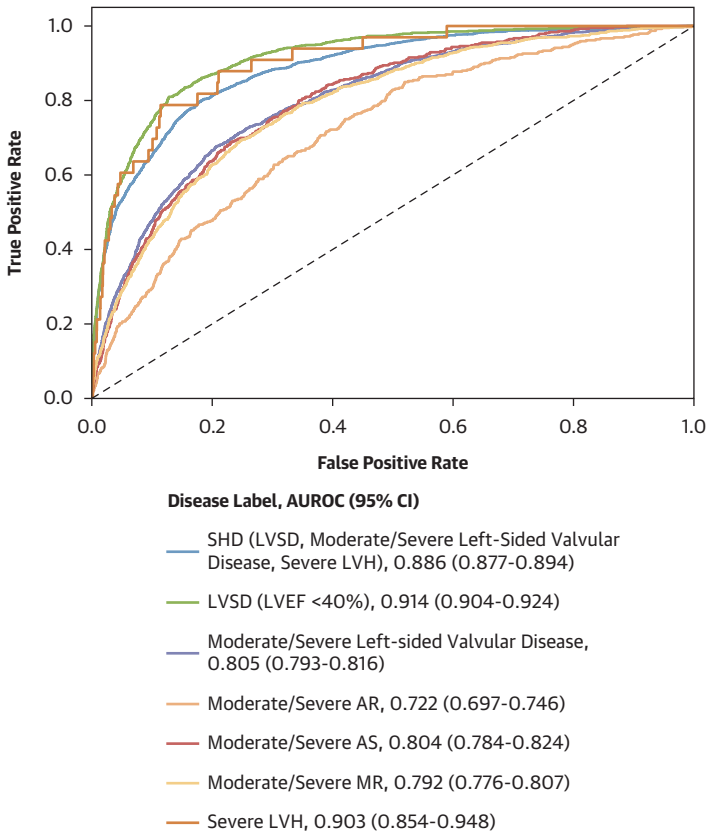

LVEF = left ventricular ejection fraction; LVH = severe left ventricular hypertrophy; other abbreviations as in Figure 1.

Although these models provide a strong foundation for the role of ECG-based detection of SHDs, their potential implementation for broad screening is limited by the low prevalence of these individual diseases and the low PPVs of the proposed models.[10-12,16,33-35] The simultaneous detection of multiple SHDs increases the composite disease prevalence and improves model precision.[19] Through a focus on detecting any of the clinically relevant SHDs that require TTE for confirmation, PRESENT-SHD enables efficient screening by limiting false discovery. Moreover, the use of ECG images as the input, and a flexible strategy that allows for varying formats, supports the scalability of the approach across resources settings.[39]

Our work has additional features that build upon the studies reported in the literature. A focus on developing PRESENT-SHD in diverse populations enabled its consistent performance in demographic subgroups across validation sites. Moreover, in addition to the accurate detection of cross-sectional disease, PRESENT-SHD also predicted the risk of new-onset disease in those without baseline SHD, representing a novel strategy for cardiovascular risk stratification. The model was well calibrated to predict the risk of SHD, suggesting that those with high PRESENT-SHD scores can benefit from surveillance, evaluation, and management of risk factors.[7,40-42]

The application of PRESENT-SHD has important implications for cardiovascular screening. Because early disease detection and intervention can alter the trajectory and outcomes of patients with SHDs, an AI-ECG-based approach that leverages ECG images and photographs can enable opportunistic screening through automated deployment across clinical settings where ECGs are obtained.[43,44] The focus on a composite model that detects a broad range of SHDs simultaneously reduces the burden of false positive screens and downstream testing, which is a major concern for AI-ECG models developed for individual cardiovascular conditions. This high PPV can allow for a sensitive threshold to be selected during implementation to identify those who should be referred for further imaging. Given that the individual components of SHD share a common diagnostic test, a TTE, screening with PRESENT-SHD can help triage the use of TTE testing. Those with a positive AI-ECG screen can be prioritized for cardiac imaging, which is especially helpful in settings where access may be limited.[1,39,45]

STUDY LIMITATIONS. First, the development population represented a selected set of patients with a clinical indication for an ECG and a TTE. The consistent validation of the model across populations with a broad range of clinical subpopulations seen in community as well as referral hospitals suggests that the model learned generalizable signatures of the SHDs. This is further supported by the consistent validation of PRESENT-SHD in the ELSA-Brasil study, where individuals underwent protocolized ECGs and echocardiograms concurrently at enrollment without any confounding by indication. Nonetheless, continued prospective validation studies are necessary before broad use in a screening population. Second, while PRESENT-SHD consistently performed well on ECG screenshots from EHR and smartphone-captured ECG photographs, it is essential to prospectively evaluate the feasibility and the performance of PRESENT-SHD in real-world settings before broad clinical adoption. Third, while we used age- and sex-matched control subjects for the development of the CNN model for sLVH detection, we did not evaluate alternative

FIGURE 3 **Cumulative Hazard for New-Onset Structural Heart Disease or Heart Failure Hospitalization in Individuals Without Structural Heart Disease or Heart Failure at Baseline**

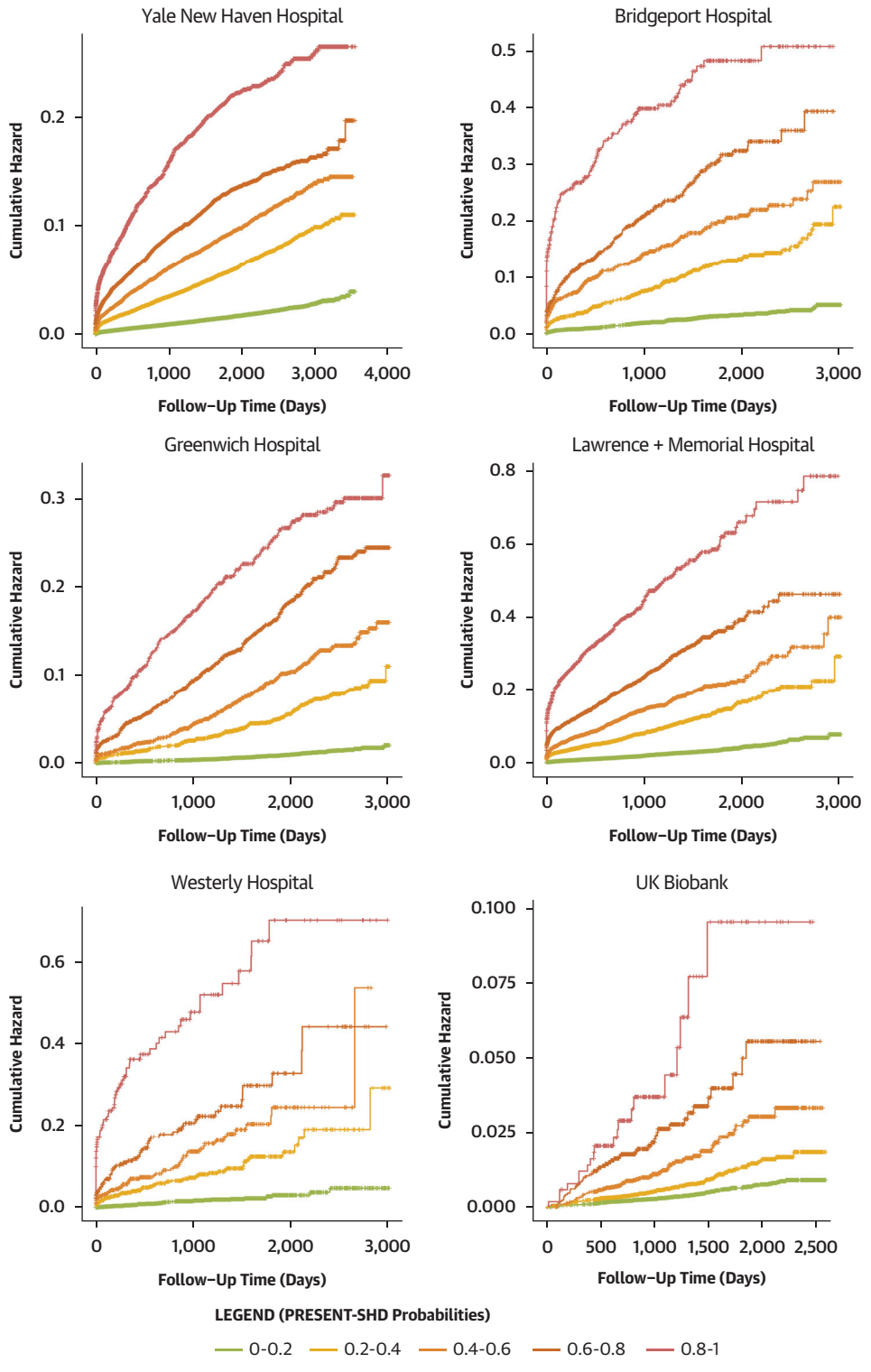

The scale of the y-axes varies across cohorts. PRESENT-SHD = Practical scREening using ENsemble machine learning sTrategy for SHD detection.

approaches that additionally use clinical risk factors for case-control matching.

Fourth, although the development of the model focused on plotted images, the signal preprocessing before image plotting represented standard steps used in ECG machines before ECG images are generated or printed. Thus, any processing of ECG images is not required for the real-world application of PRESENT-SHD, as also demonstrated in the publicly accessible application of the model. Fifth, model performance was lower in individuals aged 65 and older, potentially limiting reliability as a standalone tool to rule out the need for cardiac imaging. Adjusting model thresholds or developing age-specific models could be evaluated to improve performance. Sixth, we did not evaluate the cost-effectiveness of PRESENT-SHD use in clinical settings. However, the model had a high PPV for cross-sectional disease detection and identified individuals at high risk of developing SHD/HF, representing features favorable for deployment. Finally, in the predictive evaluation of the model, despite broad geographic coverage, some outcome events may have occurred outside the YNHH and the community hospitals, potentially resulting in incomplete capture of longitudinal outcomes. Nonetheless, the model risk stratification was consistent in the UKB, where the ECGs were protocolized and outcomes were ascertained using national EHR linkage.

CONCLUSIONS

We developed and validated a novel approach for the detection and the prediction of a range of SHDs using images of 12-lead ECGs, representing a scalable and accessible tool for SHD screening and risk stratification.

FUNDING SUPPORT AND AUTHOR DISCLOSURES

Dr Brant is supported in part by CNPq (307329/2022-4). Dr Ribeiro is supported in part by the National Council for Scientific and Technological Development - CNPq (grants 465518/2014-1, 310790/2021-2, 409604/2022-4 e 445011/2023-8). Dr Krumholz is the Editor-in-Chief of *JACC*; works under contract with the Centers for Medicare and Medicaid Services to support quality measurement programs; is associated with research contracts through Yale University from Janssen, Kenvue, and Pfizer; in the past 3 years has received options for Element Science and Identifeye and payments from F-Prime for advisory roles; and is a co-founder of and holds equity in Hugo Health, Refactor Health, and Ensight-AI. Dr Oikonomou was supported by the National Heart, Lung, and Blood Institute of the National Institutes of Health (under award F32HL170592); has been a consultant for Caristo Diagnostics Ltd and Ensight-AI Inc; and has received royalty fees from technology licensed through the University of Oxford, outside the submitted work. Drs Oikonomou and Khera are cofounders of Evidence2Health, a precision health platform to improve evidence-based cardiovascular care. Dr Khera was supported by the National Institutes of Health (under awards R01AG089981, R01HL167858, and K23HL153775) and the Doris Duke Charitable Foundation (under award 2022060); is an Associate Editor of *JAMA*; has received support from the Blavatnik Foundation through the Blavatnik Fund for Innovation at Yale; has received research support, through Yale, from Bristol Myers Squibb, BridgeBio, and Novo Nordisk; and is a coinventor of U.S. Pending Patent Applications WO2023230345A1, US20220336048A1, 63/484,426, 63/508,315, 63/580,137, 63/606,203, 63/619,241, and 63/562,335. Dr Khera and Mr Sangha are the coinventors of U.S. Provisional Patent Application No. 63/346,610, "Articles and methods for format-independent detection of hidden cardiovascular disease from printed electrocardiographic images using deep learning"; and are cofounders of Ensight-AI. The funders had no role in the design and conduct of the study; collection, management, analysis, and interpretation of the data; preparation, review, or approval of the paper; and decision to submit the paper for publication. All other authors have reported that they have no relationships relevant to the contents of this paper to disclose.

ADDRESS FOR CORRESPONDENCE: Dr Rohan Khera, Yale School of Medicine, 195 Church Street, 6th Floor, New Haven, Connecticut 06510, USA. E-mail: rohan.khera@yale.edu.

REFERENCES

1. Steinberg DH, Staubach S, Franke J, Sievert H. Defining structural heart disease in the adult patient: current scope, inherent challenges and future directions. *Eur Heart J Suppl*. 2010;12:E2-E9.

2. Picano E. Economic and biological costs of cardiac imaging. *Cardiovasc Ultrasound*. 2005;3:13.

3. Vitola JV, Shaw LJ, Allam AH, et al. Assessing the need for nuclear cardiology and other advanced cardiac imaging modalities in the developing world. *J Nucl Cardiol*. 2009;16:956-961.

4. Alkhouli M, Alqahtani F, Holmes DR, Berzingi C. Racial disparities in the utilization and outcomes of structural heart disease interventions in the United States. *J Am Heart Assoc*. 2019;8(15):e012125.

5. Samad Z, Sivak JA, Phelan M, Schulte PJ, Patel U, Velazquez EJ. Prevalence and outcomes of left-sided valvular heart disease associated with Chronic kidney disease. *J Am Heart Assoc*. 2017;6(10):e006044.

6. Fleury M-A, Clavel M-A. Sex and race differences in the pathophysiology, diagnosis, treatment, and outcomes of valvular heart diseases. *Can J Cardiol*. 2021;37:980-991.

7. Baumgartner H, Iung B, Otto CM. Timing of intervention in asymptomatic patients with valvular heart disease. *Eur Heart J*. 2020;41:4349-4356.

8. Wang TJ, Evans JC, Benjamin EJ, Levy D, LeRoy EC, Vasan RS. Natural history of asymptomatic left ventricular systolic dysfunction in the community. *Circulation*. 2003;108:977-982.

9. Galasko GI, Barnes SC, Collinson P, Lahiri A, Senior R. What is the most cost-effective strategy to screen for left ventricular systolic dysfunction: natriuretic peptides, the electrocardiogram, hand-held echocardiography, traditional echocardiography, or their combination? *Eur Heart J*. 2006;27:193-200.

10. Attia ZI, Kapa S, Lopez-Jimenez F, et al. Screening for cardiac contractile dysfunction using an artificial intelligence-enabled electrocardiogram. *Nat Med*. 2019;25:70-74.

11. Sangha V, Nargesi AA, Dhingra LS, et al. Detection of Left Ventricular Systolic Dysfunction From Electrocardiographic Images. *Circulation*. 2023;148(9):765-777. https://doi.org/10.1161/CIRCULATIONAHA.122.062646

12. Cohen-Shelly M, Attia ZI, Friedman PA, et al. Electrocardiogram screening for aortic valve stenosis using artificial intelligence. *Eur Heart J*. 2021;42:2885-2896.

13. Bjerkén LV, Rønborg SN, Jensen MT, Ørting SN, Nielsen OW. Artificial intelligence enabled ECG screening for left ventricular systolic dysfunction: a systematic review. *Heart Fail Rev*. 2023;28:419–430.

14. Khunte A, Sangha V, Oikonomou EK, et al. Detection of left ventricular systolic dysfunction from single-lead electrocardiography adapted for portable and wearable devices. *NPJ Digit Med*. 2023;6:124.

15. Oikonomou EK, Sangha V, Dhingra LS, et al. Artificial intelligence-enhanced risk stratification of cancer therapeutics-related cardiac dysfunction using electrocardiographic images. *Circ Cardiovasc Qual Outcomes*. 2025;18(1):e011504.

16. Sangha V, Dhingra LS, Oikonomou EK, et al. Identification of hypertrophic cardiomyopathy on electrocardiographic images with deep learning. *medRxiv*. 2023, 2023.12.23.23300490.

17. Dhingra LS, Sangha V, Aminorroaya A, et al. A multicenter evaluation of the impact of procedural and pharmacological interventions on deep learning-based electrocardiographic markers of hypertrophic cardiomyopathy. *bioRxiv*. Published online January 2024. https://doi.org/10.1101/2024.01.15.24301011

18. Dhingra LS, Aminorroaya A, Camargos AP, et al. Using artificial intelligence to predict heart failure risk from single-lead electrocardiographic signals: a multinational assessment. *bioRxiv*. 2024, 2024.05.27.24307952.

19. Ulloa-Cerna AE, Jing L, Pfeifer JM, et al. rECHOmmend: An ECG-Based Machine Learning Approach for Identifying Patients at Increased Risk of Undiagnosed Structural Heart Disease Detectable by Echocardiography. *Circulation*. 2022;146:36–47.

20. CarDS LAB. Yale School of Medicine. PRESENT-SHD. Accessed February 7, 2025. https://www.cards-lab.org/present-shd

21. Mitchell C, Rahko PS, Blauwet LA, et al. Guidelines for performing a comprehensive transthoracic echocardiographic examination in adults: Recommendations from the American society of echocardiography. *J Am Soc Echocardiogr*. 2019;32:1–64.

22. Zoghbi WA, Adams D, Bonow RO, et al. Recommendations for noninvasive evaluation of native valvular regurgitation: a report from the American society of echocardiography developed in collaboration with the society for cardiovascular magnetic resonance. *J Am Soc Echocardiogr*. 2017;30:303–371.

23. Zoghbi WA, Adams D, Bonow RO, et al. Recommendations for noninvasive evaluation of native valvular regurgitation. *J Indian Acad Echocardiogr Cardiovasc Imaging*. 2020;4:58–121.

24. Kossaify A, Nasr M. Diastolic dysfunction and the new recommendations for echocardiographic assessment of left ventricular diastolic function: summary of guidelines and novelties in diagnosis and grading. *J Diagn Med Sonogr*. 2019;35:317–325.

25. Pillow 11.1.0. PyPI. Accessed February 29, 2024. https://pypi.org/project/pillow/

26. Tan M, Le QV. EfficientNet: rethinking model scaling for convolutional neural networks. *International Conference on Machine Learning*. 2019. arXiv:1905.11946v5.

27. Sangha V, Khunte A, Holste G, et al. Biometric contrastive learning for data-efficient deep learning from electrocardiographic images. *J Am Med Inform Assoc*. 2024;31(4):855–865. https://doi.org/10.1093/jamia/ocae002

28. Austin PC, Fine JP. Practical recommendations for reporting Fine-Gray model analyses for competing risk data. *Stat Med*. 2017;36:4391–4400.

29. Uno H, Cai T, Pencina MJ, D'Agostino RB, Wei LJ. On the C-statistics for evaluating overall adequacy of risk prediction procedures with censored survival data. *Stat Med*. 2011;30:1105–1117.

30. Kang L, Chen W, Petrick NA, Gallas BD. Comparing two correlated C indices with right-censored survival outcome: a one-shot nonparametric approach. *Stat Med*. 2015;34:685–703.

31. TRIPOD+AI statement: updated guidance for reporting clinical prediction models that use regression or machine learning methods. *BMJ*. 2024;385:q902.

32. Ko W-Y, Siontis KC, Attia ZI, et al. Detection of Hypertrophic Cardiomyopathy Using a Convolutional Neural Network-Enabled Electrocardiogram. *J Am Coll Cardiol*. 2020;75:722–733.

33. Goto S, Solanki D, John JE, et al. Multinational federated learning approach to train ECG and echocardiogram models for hypertrophic cardiomyopathy detection. *Circulation*. 2022;146:755–769.

34. Grogan M, Lopez-Jimenez F, Cohen-Shelly M, et al. Artificial intelligence-enhanced electrocardiogram for the early detection of cardiac amyloidosis. *Mayo Clin Proc*. 2021;96:2768–2778.

35. Taborsky M, Aiglova R, Fedorco M, et al. Detection of arrhythmias in patients with cardiac amyloidosis using implantable ECG recorders. *Eur Heart J*. 2022;43.

36. Duong SQ, Vaid A, Vy HMT, et al. Quantitative prediction of right ventricular and size and function from the electrocardiogram. *medRxiv*. 2023. Published online April 26, 2023. https://doi.org/10.1101/2023.04.25.23289130

37. Vaid A, Johnson KW, Badgeley MA, et al. Using deep-learning algorithms to simultaneously identify right and left ventricular dysfunction from the electrocardiogram. *JACC Cardiovasc Imaging*. 2022;15:395–410.

38. Oikonomou EK, Sangha V, Shankar SV, et al. Tracking the pre-clinical progression of transthyretin amyloid cardiomyopathy using artificial intelligence-enabled electrocardiography and echocardiography. *bioRxiv*. 2024;2024, 08.25.24312556.

39. Mocumbi AO. Cardiovascular health care in low- and middle-income countries. *Circulation*. 2024;149:557–559.

40. Tarakji KG, Brunken R, McCarthy PM, et al. Myocardial viability testing and the effect of early intervention in patients with advanced left ventricular systolic dysfunction. *Circulation*. 2006;113:230–237.

41. Ullah W, Gowda SN, Khan MS, et al. Early intervention or watchful waiting for asymptomatic severe aortic valve stenosis: a systematic review and meta-analysis. *J Cardiovasc Med (Hagerstown)*. 2020;21:897–904.

42. Levin A, Singer J, Thompson CR, Ross H, Lewis M. Prevalent left ventricular hypertrophy in the predialysis population: identifying opportunities for intervention. *Am J Kidney Dis*. 1996;27:347–354.

43. Topol E, Opportunistic AI. *for medical scans. Ground Truths*. 2024. Accessed July 28, 2024. https://erictopol.substack.com/p/opportunistic-ai-for-medical-scans

44. Jelinek H, Warner P, King S, De Jong B. Opportunistic screening for cardiovascular problems in rural and remote health settings. *J Cardiovasc Nurs*. 2006;21:217–222.

45. Diamantino AC, Nascimento BR, Nunes MCP, et al. Impact of incorporating echocardiographic screening into a clinical prediction model to optimise utilisation of echocardiography in primary care. *Int J Clin Pract*. 2021;75:e13686.

KEY WORDS artificial intelligence, cardiovascular screening, deep learning, echocardiography, electrocardiograms, predictive modeling, structural heart disease

APPENDIX For an expanded Methods section as well as supplemental figures and tables, please see the online version of this paper.